Geophysica (1989), **25**, 1&2, 1–20

Ten Year Summary 1977–1986 of Atmospheric Electricity Measured at Helsinki-Vantaa Airport, Finland

Tapio J. Tuomi

Finnish Meteorological Institute
P.O. Box 503, SF–00101 Helsinki, Finland

Abstract

Continuous recording of atmospheric electric parameters at ground level at Helsinki-Vantaa Airport, Finland, is summarized for the ten-year period 1977–86. The yearly, seasonal and diurnal variations of the fair-weather hourly means of potential gradient (downward electric field), air-earth current density and the positive- and negative-ion components of conductivity are presented. The mutual consistency of these parameters is checked with Ohm's law, which holds within 90%; the long-term variations of the deviation from Ohm's law are very small. The Chernobyl deposition caused a tenfold increase in conductivity in May 1986; the normal level was again reached by the end of summer 1986. A rough comparison between the measured conductivity and the visibility reported at the site is made in terms of aerosol models. The results suggest that despite the air traffic, the fraction of smallest particle sizes remains low, which means that the main part of the aerosol is aged and gives rise to grey rather than blue haze.

1. *Introduction*

The most traditional area of interest in atmospheric electricity is perhaps *fair-weather electricity*, which covers the study of quasi-stationary electrical phenomena outside thunderstorms and other disturbed regions in the lower and middle atmosphere. It is closely associated with cosmic radiation, radioactivity and aerosols. The basic quantities of fair-weather electricity, the electric field, current density and conductivity near the ground, are subject to both global and local variations. Global variations are associated with tropical thunderstorms and upper-atmospheric effects and cannot be easily evaluated from the data of a single ground-level measuring station. Local influences are more readily at hand and will be discussed in some detail.

The ground-level electric field was measured in Finland (Helsinki) near the turn of the century for a period of about twenty years (*Lemström*), and later there was a

recording period (unpublished) in Sodankylä, Northern Finland. A new measurement period, still continuing, started in 1976 at Helsinki-Vantaa Airport with automatic continuously running instruments; digital data are available since May 1977. Another station was set up in the northernmost part of Finland in the 1980s but its results are not presented here. The measuring station and instruments are described in *Tuomi* (1988), which also includes a list of the yearbooks where the hourly values have been published.

The purpose of this work is to give a review of the atmospheric electric "climate" of Southern Finland in terms of such average properties as yearly, seasonal and diurnal variations of the measured parameters (Secs. 4–6). Deep physical analyses cannot be made because of the lack of information of related parameters such as aerosol size distributions and concentrations, *etc.*, but studies which have used the measured data will be mentioned briefly in addition to an introductory theoretical discussion (Sec. 2). A parameter available at the measuring site is visibility, and an attempt to derive average properties of the aerosol from a comparison of visibility with conductivity is made in Sec. 3. The role of conductivity as an indicator of local air pollution is considered in terms of its weekly variation in Sec. 7.

The most pronounced atmospheric electric effect during the period 1977–86 was caused by the Chernobyl nuclear power plant accident in April 1986; it is described in Sec. 8.

2. *Ground-level atmospheric electricity*

The region of interest in the present work is depicted in Fig. 1 as a part of the global circuit, which is mainly generated by about 1500 tropical thunderstorms, each of which charges the upper atmosphere (at about 100 km and above) by a current of the order of 1A. The upper atmosphere acquires a potential of about 300 kV with respect to the ground, called the ionospheric potential; this drives the downward fair-weather current which is distributed over the atmosphere according to the vertical columnar resistance. The electrical conductivity of air is about 20 fS/m within the lowest one or two kilometres and its magnitude is mainly determined by the aerosol content. Above this mixing layer, conductivity grows roughly exponentially, increasing tenfold every 10 km increase of height. Up to about 80 km, conductivity is isotropic, becoming anisotropic higher up where the relatively free electrons and ions are influenced by the Earth's magnetic field. The average columnar resistance, most of which is due to the mixing layer, is about $1.5 \cdot 10^{17}\ \Omega m^2$, hence the ionospheric potential drives a fair-weather current density of about $2\ pA/m^2$.

At a ground-level fair-weather measuring station, current density is the quantity most clearly related to the global circuit although it is also controlled by the regionally

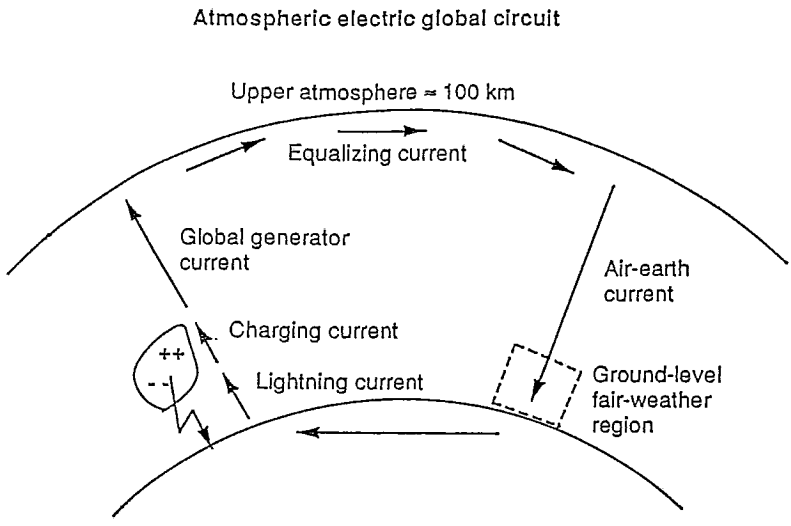

Fig. 1. The most important elements of the atmospheric electric global circuit. The source of the circuit is the charging current of thunderclouds, caused by a thermodynamic charge separation mechanism which is not yet fully understood.

variable lower part of the columnar resistance. A discussion of the averages and variations of the current density is given by *Israel* (1973).

The quantity of the most local nature is conductivity, which is practically solely caused by the drift of small ions which originate from molecules in the air ionized by cosmic radiation and local radioactivity. The principal small ions are clusters of a few water molecules around a proton (*i.e.*, the H^+ ion) or around O_2^- or CO_4^-. Their electrical mobility k is about $1.2 \cdot 10^{-4}$ m^2/Vs; the conductivity λ is the sum of a positive-ion and a negative-ion component

$$\lambda = \lambda^+ + \lambda^- = ke(n^+ + n^-) \qquad (1)$$

where n^+ and n^- are the small-ion densities (m^{-3}) and e is the elementary charge. Under normal conditions, the small-ion densities are nearly equal ($= n$), and the simplest possible equation describing the balance between ionization, small ions and aerosol is as follows:

$$q = \alpha n^2 + \beta n N \qquad (2)$$

where q is the ionization (m^{-3}s^{-1}), α is the small-ion recombination coefficient (about $1.6 \cdot 10^{-12}$ m^3/s), β ($\approx \alpha$) is the ion-aerosol attachment coefficient and N is the aerosol

density (m^{-3}), assumed to be a representative value for the small-particle part of the aerosol size spectrum. The aerosol quantities β and N will be discussed more in the next section.

If there are no convection currents, the globally controlled current density i and the local conductivity λ are related to the electric field E according to Ohm's law:

$$i = \lambda E. \tag{3}$$

The four quantities, current density, electric field and the two components of conductivity, form the basic set to be measured at a ground-level atmospheric electric station.

Before going to the presentation of the results, it is instructive to look at the above equations in view of the average values. The ten-year means of the four measured quantities are

$$i = 2.80 \text{ pA/m}^2 \tag{4}$$
$$E = 204 \text{ V/m} \tag{5}$$
$$\lambda^+ = 9.1 \text{ fS/m} \tag{6}$$
$$\lambda^- = 8.5 \text{ fS/m} \tag{7}$$

which have been calculated from the hourly fair-weather means (the number of hours was 32,000 out of 85,000 possible). The fulfilment of Ohm's law has been tested for each hour (actually for each 10 min), and the ten-year average of the current ratio $\Omega = i/\lambda E$ (ratio of measured current density to conduction current density) is

$$\Omega = 0.89; \tag{8}$$

the value calculated from the long-term values (4)–(7) is 0.78, the difference reflecting the nonlinearity of the expression of Ω. The fact that the average Ω is smaller than unity could be associated with the electrode effect (the depletion of negative ions near the ground), but this is not certain (see *Tuomi*, 1982).

Reasonable estimates of the average ionization rate are $5.6 \cdot 10^6$ $m^{-3}s^{-1}$ (10.2 μR/h) for cosmic radiation and terrestrial gamma radiation, and 10^6 $m^{-3}s^{-1}$ (1.8 μR/h) for radon activity in the air, totalling $6.6 \cdot 10^6$ $m^{-3}s^{-1}$ (12 μR/h). The measured conductivity gives a small-ion density of either sign of about $4.5 \cdot 10^8$ m^{-3}, and hence the aerosol density in (2) becomes $N = 8.7 \cdot 10^9$ m^{-3}, *i.e.* about twenty times the small-ion density (more refined estimates of these quantities will be given in the next section). Because of the attachment of small ions, about one half of the aerosol particles are neutral and one fourth is positive, one fourth negative (see *e.g. Tuomi*, 1981).

3. *Correlation between conductivity and visibility*

Because the measurement site is at an airport, visibility data, among other meteorological data, are available. In the following, a comparison is made between visibility and positive conductivity. This will give an insight into the nature of the atmospheric aerosol, which is an essential factor in the atmospheric electrical climate.

Visibility is the maximum distance at which large, well-contrasting objects can be seen through the atmosphere. It is defined as

$$V = 3.9/a \tag{9}$$

where a is the extinction coefficient (m^{-1}) of the atmosphere for visible light (see *e.g. Fleagle & Businger*, 1963, p. 277). The extinction coefficient is normally the sum of a Rayleigh-scattering term due to the atmospheric gas, $a_R = 0.016$ km^{-1}, and an aerosol term $N\sigma$,

$$a = a_R + N\sigma \tag{10}$$

where σ is the average extinction cross-section (m^2) of an aerosol particle. If the cross section remains constant under varying visibility conditions, as might be expected if misty (high-humidity) periods are excluded, eqs. (2), (9) and (10) suggest that visibility and conductivity are nearly linearly correlated (when αn^2 and a_R are neglected). However, a comparison with data from representative periods in May 1979 and May 1981, using fair-weather hours with relative humidity below 70% and local radioactivity at a low level, gives the average dependence

$$\lambda^+(\mathrm{fS/m}) = 3.08(V(\mathrm{km}))^{1/4}. \tag{11}$$

It should be stressed that this is a very rough relation; for a given value of visibility, the conductivity has a scatter of about 2 fS/m around the mean for this particular period. There are also periods for which the proportionality factor is different. Certain properties of the aerosol can be estimated by examining how Eq. (11) can be satisfied by reasonable aerosol models.

The most important property of an aerosol is its size distribution, which is highly variable but is generally dominated (by number) by particles with radius r of the order of 0.1 μm (spherical particles will be assumed here). Although many refined size-distribution models have been developed, the classic power-law model of *Junge* (1963)

$$N(r) = \nu N r_1^{\nu} r^{-\nu-1} \tag{12}$$

where $r_1 \leq r \leq r_2$ and $r_2 >> r_1$, is still useful because of its simplicity: it has only one parameter ν (usually between 2.5 and 4.0) if the lower and upper size limits are kept fixed. Usual choices are $r_1 = 0.04$ μm and $r_2 = 10$ μm. The sharp cut at r_1 can be smoothed by the modified distribution

$$\begin{aligned} N(r) &= N r_1^{-1} && r_1/\nu \leq r \leq r_1 \\ N(r) &= N r_1^{\nu} r^{-\nu-1} && r_1 \leq r \leq r_2 \end{aligned} \tag{13}$$

Consider first the Junge distribution (12). The ion-aerosol attachment coefficient $\beta(r)$ is nearly linear in r and can be approximated by

$$\beta(r) = 4.36 \cdot 10^{-5} r - 9.2 \cdot 10^{-14} \tag{14}$$

in units of 10^{-12} m^{3}s^{-1} when r is expressed in metres (*Hoppel*, 1985). The slightly simpler expression $\beta(r) = 4.2 \cdot 10^{-5} r$ will be used here. For a Junge distribution, the average radius is $\nu r_1/(\nu-1)$, which for $r_1 = 0.04$ μm would give the average attachment coefficient $\beta = 2.5 \cdot 10^{-12}$ m^{3}s^{-1} for $\nu = 3$. This is somewhat larger than most values quoted in the literature for continental aerosols (see *e.g. Hoppel*, 1985, for a discussion), and the lower radius $r_1 = 0.03$ μm will be assumed for distribution (12). For the modified distribution (13), $r_1 = 0.04$ μm gives good results.

Extinction cross-sections computed for Junge aerosols are available in the literature, and the results of *McCormick et al.* (1968) for refractive index 1.5 will be used. It turns out that the extinction cross-section for wavelength Λ (assumed here 0.55 μm) can be expressed in the form

$$\sigma = \nu (2\pi r_1/\Lambda)^{\nu} (\Lambda/2\pi)^2 I(\nu) \tag{15}$$

where $I(\nu)$ is almost independent of parameters other than ν and can be approximated by

$$I(\nu) = 33(\nu-1)^{-2.5}. \tag{16}$$

If the modelled attachment coefficient and extinction cross-section are used with the average relation (11), a correspondence between V and ν as given in Table 1 is obtained. The resulting extinction cross sections and aerosol number densities are also given. The most striking feature in Table 1 is the low value of ν, which is well below the "standard" value 3.0. This is partly caused by the small value of r_1 required by the attachment coefficient.

Table 1. Relation of visibility to various aerosol parameters; Junge model.

V (km)	ν	σ (10^{-14} m^2)	N (10^9 m^{-3})
10	2.14	3.94	9.6
20	2.38	2.10	8.7
30	2.55	1.40	8.2
40	2.68	1.05	7.8
50	2.79	0.83	7.5

Thus Table 1 demonstrates that on the average, good visibility is associated with small particles (σ small and ν large), bluish haze (large ν; small value means grey haze) and low aerosol content (N small). Such conditions often prevail when the air mass comes from the north. However, the fact that even the largest value of ν is below 3 indicates that the typical Finnish aerosol is aged, *i.e.* the smallest particles have been coagulated out, and its colour is grey. Larger values of ν would be obtained under conditions of at least moderate visibility with blue haze and low conductivity. However, blue haze, usually associated with warm continental air mass, occurs rather rarely. The above conclusions do not depend critically on the relation (11).

If the modified size distribution (13) is assumed, the extinction cross-sections of *McCormick et al.* (1968) can be used for $r \geq r_1$, and for the small-particle part the cross-section can be calculated by using the Rayleigh-scattering approximation

$$\sigma_R(r) = \pi r^2 (8/3)(2\pi r/\Lambda)^4 ((m-1)/(m+2))^2 \qquad (17)$$

where m is the index of refraction (see *e.g. Van de Hulst*, 1957). Application of the relation (11) to the latter aerosol model, which should be considered more realistic, gives the results shown in Table 2.

Table 2. Relation of visibility to various aerosol parameters; modified model.

V (km)	ν	σ (10^{-14} m^2)	N (10^9 m^{-3})
10	2.14	3.41	10.7
20	2.37	1.80	10.0
30	2.55	1.15	9.6
40	2.66	0.89	9.2
50	2.77	0.69	9.0

The values of ν are almost the same as in the Junge model. Because smaller particles are included in the modified model, the average cross-sections are naturally smaller and the particle numbers higher.

4. *Year-to-year variations*

The yearly means of the four measured quantities are shown in Fig. 2, which also contains the current ratio Ω, calculated for each hour before averaging. The current density (positive downward) and the potential gradient (downward electric field) remain relatively constant; evaluation of the significance of the variations would require comparisons with other stations. The conductivities show rather great variations which are also difficult to explain without detailed measurements of other atmospheric-physical parameters. For example, air traffic near the measurement site has some influence on the conductivity, and part of the general decrease may be caused by the increased number of flights. The sharp rise in 1986, on the other hand, is due to the Chernobyl deposition. The negative conductivity lies always slightly below the positive one. Comparisons of the conductivity with measurements of the total suspended matter (due mainly to the coarser fraction of the aerosol) within 20 km of the site have been attempted, but the correlations are generally poor.

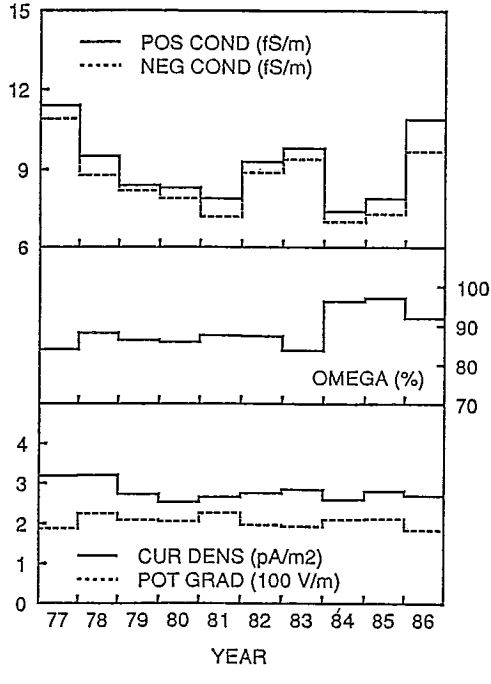

Fig. 2. Year-to-year variations of the atmospheric electric parameters.

The current ratio (omega) remains rather constant below 0.9 except for 1984 and 1985, there being an apparent negative correlation with conductivity. However, such a correlation is not present in the month-to-month variations within these years nor, for that matter, within any other year. The variations of the current ratio are mostly irregular though its fair-weather hourly means normally remain between 0.5 and 1.2 at this particular site. The above mentioned correlation could also have been caused by slight contamination (blocking) of the grids protecting the inlets of the instrument, but the inlets are kept unprotected during winter, and no seasonal differences in the correlation can be found.

5. *Seasonal variations*

Fig. 3 shows the month-to-month variation of the current density. The same pattern, *i.e.* smaller values in summer, is present in individual years (not shown) and is probably mainly caused by seasonal variations in the global thunderstorm activity, which has its maximum in southern-hemisphere summer.

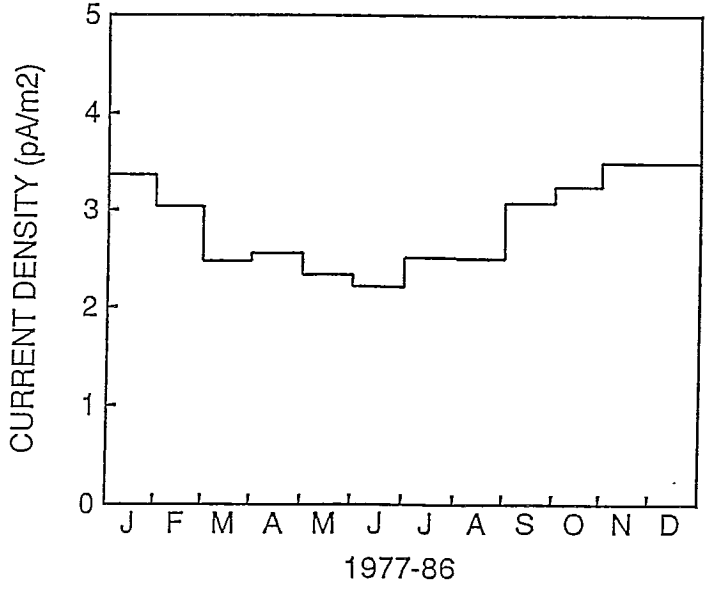

Fig. 3. Monthly means of current density.

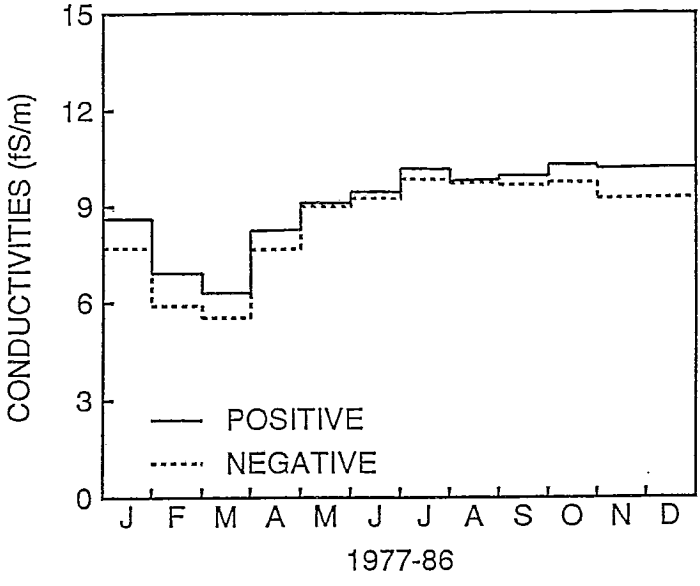

Fig 4. Monthly means of the two components of conductivity.

The seasonal variation of the conductivities is shown in Fig. 4. A feature worth noting is a minimum in winter, probably caused partly by snow which attenuates the gamma radiation from the ground, and partly by high aerosol content associated with springtime temperature inversions. Another feature is the difference between positive and negative conductivity, which is greatest in winter and almost nil in summer. This difference has been separately studied and found to be associated with the electrode effect (*Tuomi*, 1981, 1982). The difference remains similar even within individual hours while the conductivities themselves show great variations. It should be stressed here that the two components of conductivity are always very close to one another during fair weather except for the small difference due to the electrode effect.

Great differences between the conductivity components in the present site have always been associated with charged overhead clouds (with or without precipitation) or instrumental faults such as short-circuiting by spider's webs or blocking of air inlets by frost. A small average difference for randomly chosen periods from various places is also reported by *Israel* (1970, p. 95), with an average conductivity ratio of $\lambda^+/\lambda^- = 1.15$. On the other hand, there are reports in which there are large fair-weather differences between the conductivity components. For instance, *Ungethüm et al.* (1974) have found in Uppsala, Sweden, not very far from the present site, that the monthly means of the

conductivity ratio vary between 0.5 (in summer) and 2 (in winter). The highest values of λ^- with respect to λ^+ occur at night in summer. A report from Italy (*Cerquetti*, 1988) gives the 1987 average diurnal curve where λ^- is also larger than λ^+, the difference being very large at night and varying strongly during the day.

The potential gradient, although influenced locally by conductivity, is the most frequently discussed parameter of those presented here, probably because it was the first quantity measured in atmospheric electricity. The month-to-month patterns in individual years (not shown) are remarkably similar to the average curve shown in Fig. 5, even to a larger extent than the more global parameter current density. *Israel* (1973, p. 353) shows several curves of the annual (seasonal) variation of the potential gradient, which exhibits an almost perfect sinusoidal variation with the minimum in June or July. The same variation can be seen in Fig. 5, modulated, however, by the conductivity minimum in January-April.

The current ratio Ω (Fig. 6) does not show any significant pattern. Its irregular variations seem to be random over long term and average out almost completely.

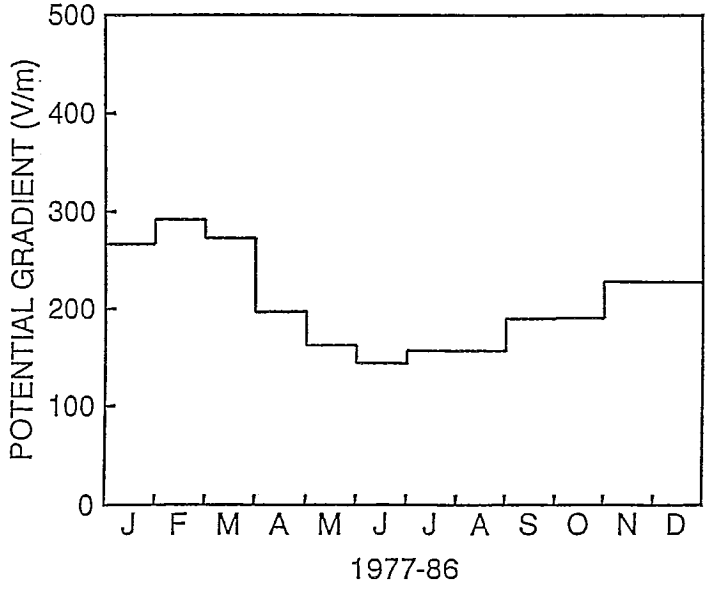

Fig. 5. Monthly means of potential gradient.

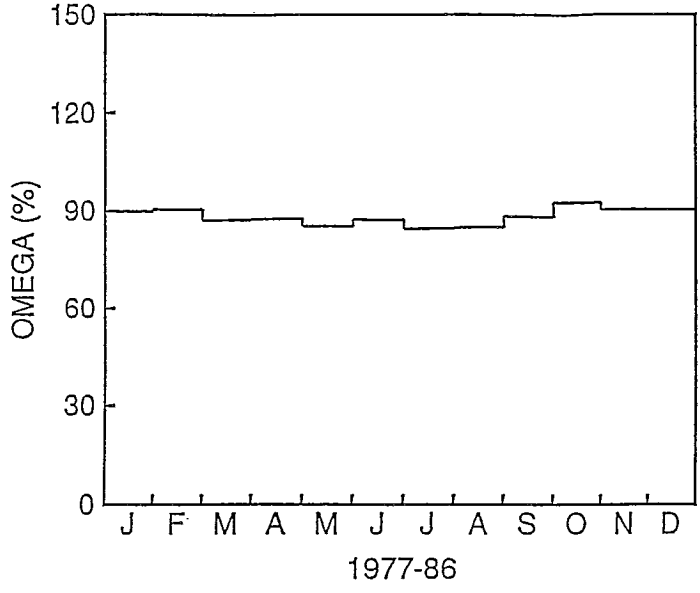

Fig. 6. Monthly means of the current ratio Ω.

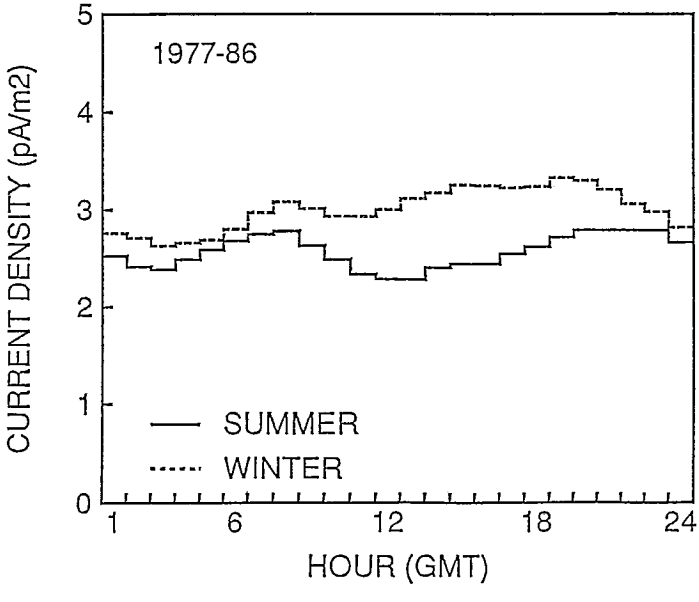

Fig. 7. Diurnal variation of current density.

6. *Diurnal variations*

The diurnal variations are the most frequently presented ones in the literature, and therefore comparisons with published results can be made best. The present data have been divided into two seasons, a "summer" (May-October) and a "winter" (November-April), which are roughly distinguished by the presence of permanent snow cover. The maximum snow depth, about 40 cm on the average, is reached near the end of February.

Current density (Fig. 7) is characterized by a minimum in the morning (in GMT; the local time is normally GMT + 2h, but since 1981 it has been GMT + 3h from April to September, which coincides with most of the summer defined above). In summer, there is a noon (local afternoon) minimum which is almost absent in winter; these features are similar each year. *Israel* (1973, p. 488–496) gives many examples of the diurnal variation of current density and discusses its causes. Israel's main conclusions are that the diurnal-variation pattern may be quite different for different stations, and that the most important factor in this respect is the columnar resistance.

The conductivities (Figs. 8 and 9) are highest at night and lowest in the afternoon when the aerosol burden from mixing and traffic is heaviest; this will be discussed in greater detail in Section 7. The electrode-effect difference in the two components of conductivity is almost constant during the day.

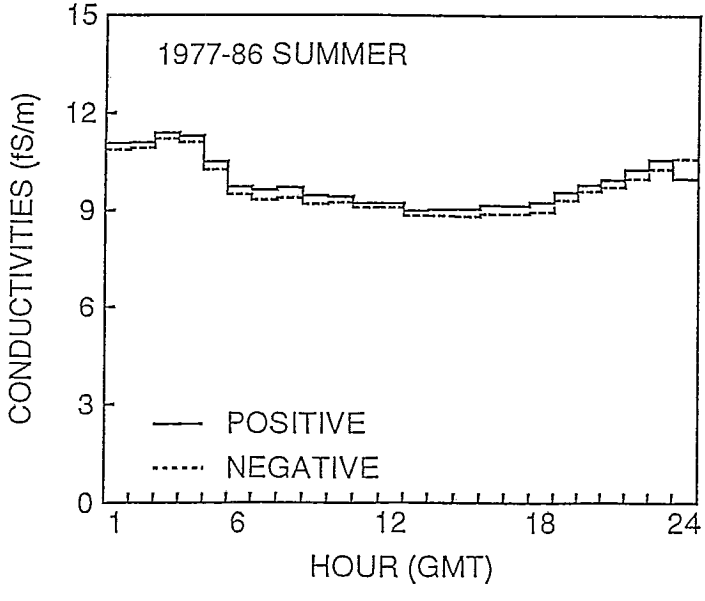

Fig. 8. Diurnal variation of conductivity in summer.

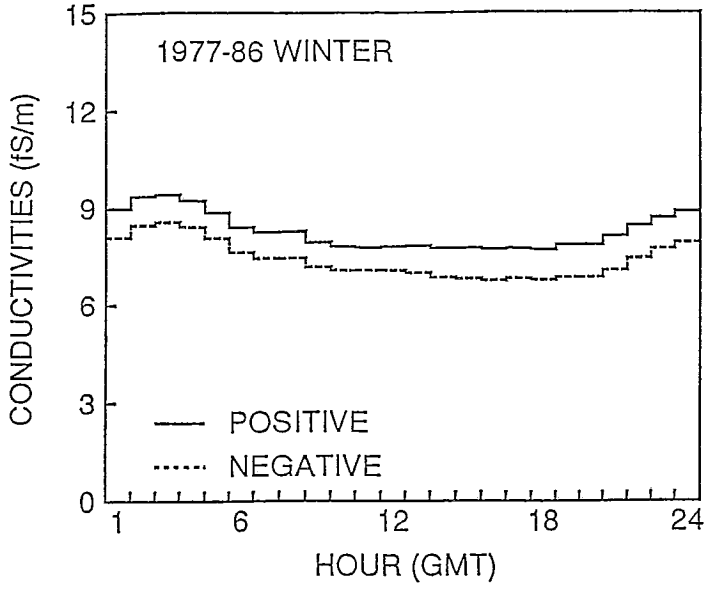

Fig. 9. Diurnal variation of conductivity in winter.

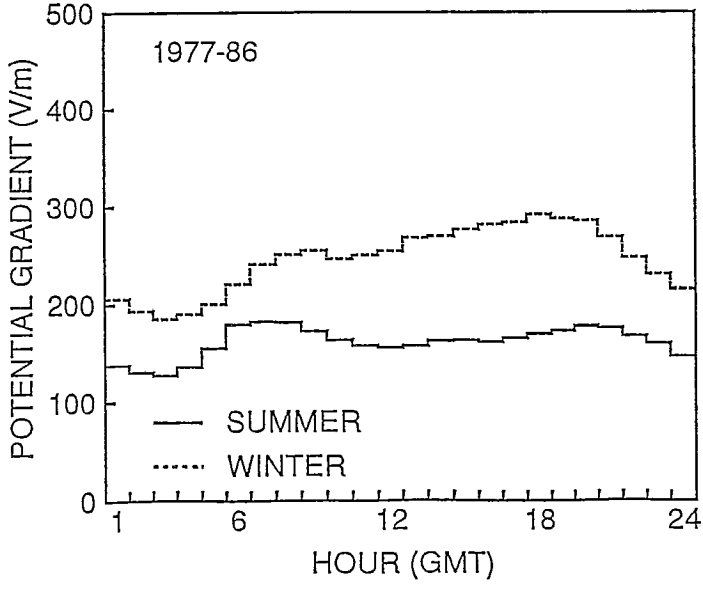

Fig. 10. Diurnal variation of potential gradient.

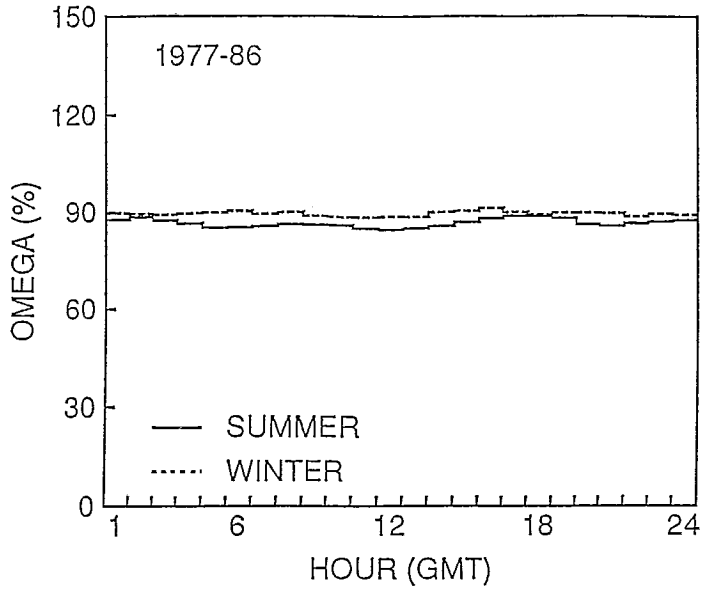

Fig. 11. Diurnal variation of the current ratio Ω.

Potential gradient (Fig. 10) has a similar difference between the summer and winter patterns as current density. *Israel* (1973, p. 346–351) presents similar seasonal differences in other stations, too. The winter pattern is rather close to the variation found over oceans and above the mixing layer while the summer pattern is typical of the mixing layer on continents.

The diurnal variation of Ω (Fig. 11) is as small as its seasonal variation.

7. *Weekly variation of conductivity*

Man's activity in increasing the aerosol content of the atmosphere has many easily distinguishable periodicities: the daily rush hours, the less active weekends, and, at least in cold climates, summer-winter variations in the production of smoke from heating-power plants. The most obvious source of aerosol in the present site is air traffic, which has a similar periodicity as the urban car traffic around. The effects of the variations in the total traffic should be reflected in the electrical parameters, most directly in conductivity. An additional factor is provided by the change of local time (LT) by one hour during summers since 1981. Fig. 12 shows the diurnal variation of positive conductivity

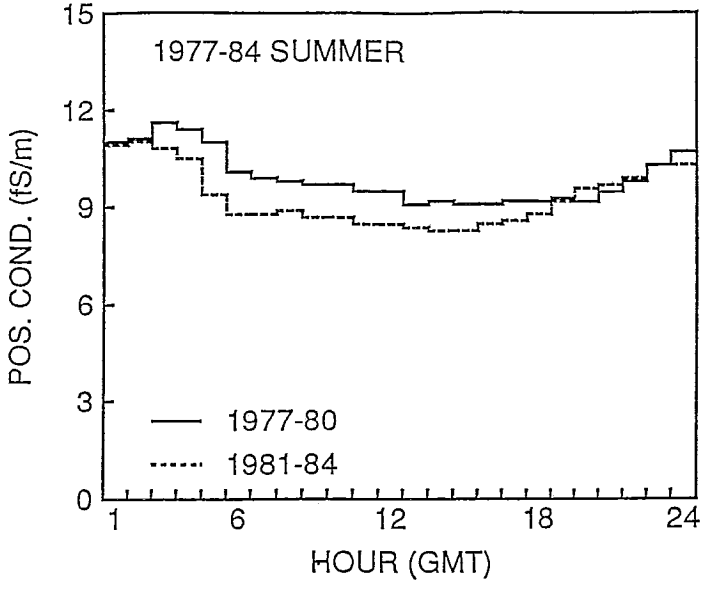

Fig. 12. Diurnal variation of the summertime positive conductivity during two periods representing the normal local time (GMT + 2h until 1980) and the daylight-saving time (GMT + 3h since 1981).

for summer, separately for 1977–80 (LT = GMT + 2h) and 1981–84 (LT = GMT + 3h). It is clearly seen that the morning-rush decrease of conductivity has shifted one hour earlier with the change of local time.

The same shift is seen in the Monday-Friday curves of Fig. 13, where the weekdays and weekend are plotted separately. The one-hour shift seems to be present in the Saturday-Sunday curves also, but this cannot be concluded with certainty because the sharp rush-hour decrease is now lacking.

8. *The Chernobyl deposition*

On April 26, 1986, there was an explosion in the Chernobyl power plant in the Soviet Union. Radioactive matter, mainly $_{53}I^{131}$ and $_{55}Cs^{137}$, was transported to Finland, among other countries, at a height of 1..2 km and was deposited with precipitation. According to a map constructed by the Finnish Centre for Radiation and Nuclear Safety, the Helsinki area was in a low-deposition region of less than 3 kBq/m^2 while the highest values in Finland were about 60 kBq/m^2. The amount of precipitation at the

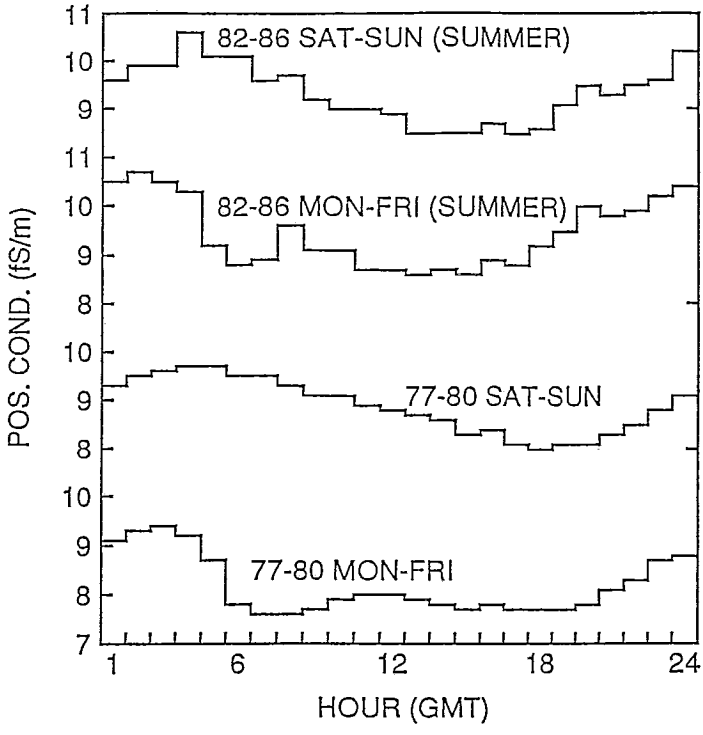

Fig. 13. Diurnal variation of positive conductivity during representative periods similar to those in Fig.12, separately for weekdays (Mon-Fri) and weekend (Sat-Sun).

electrical measurement site is not known because of a strike at the time of the deposition, but the sharp rise of conductivity indicates that there was a local shower. Fig. 14 illustrates the situation, showing hourly means (GMT) of the total conductivity and the conduction current density calculated from the conductivity and the electric field. The first indication of high radioactivity in the air is seen on 28 April when subsiding air brought radioactive matter, mostly iodine, temporarily close to the ground as a dry deposition. Precipitation occurred on the afternoon of 29 April, rising the conductivity out of scale; this was not realized until 2 May when a routine service call was made and a proper scale was selected. The conductivity rise was also indirectly seen in the electric field (not shown), which was almost short-circuited down to values below 20 V/m, *i.e.* to about one tenth of the normal level. Measurement of current density suffered from technical faults, but the calculated current density in Fig. 14 remains, on the average, fairly well at the normal level although it is more "noisy" than usually. Many of the peaks in current density and conductivity correlate, suggesting that the conductivity variations are associ-

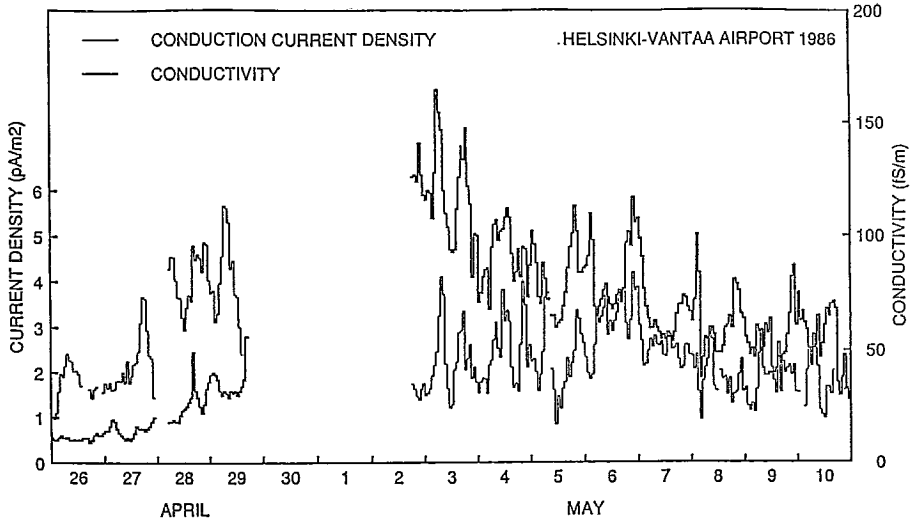

Fig. 14. Effect of the Chernobyl deposition on the conductivity and the conduction current density.

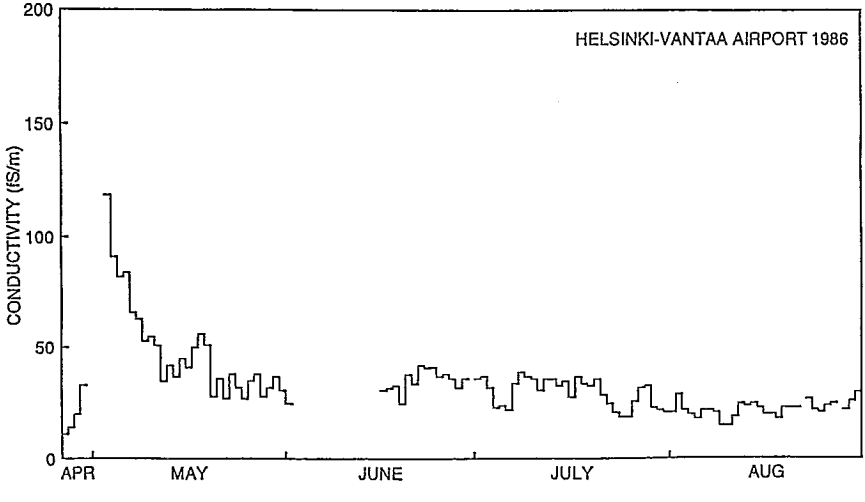

Fig. 15. Return of the conductivity close to normal after the Chernobyl deposition.

ated with significant variations in the whole columnar resistance of the atmosphere.

As can be seen in Fig. 14, there was a rather rapid decrease of conductivity after the main deposition, reflecting the high proportion of $_{53}I^{131}$, which has a half-life of eight days. The remaining activity, mainly due to cesium which has a half-life of 30 years, prevailed until the latter half of July (Fig. 15). At the end of the unusually dry summer there was a lot of precipitation, dissolving most of the deposited material deeper into the ground. Already in August the conductivity level was quite normal.

Very similar effects on atmospheric electrical parameters were observed by *Israelsson and Knudsen* (1986) in Uppsala, Sweden.

9. *Conclusions*

Summary of the first ten years (May 1977 – December 1986) of atmospheric electricity recording at Helsinki-Vantaa Airport, Finland, is given. The averages of the recorded current density, positive and negative conductivity, and potential gradient at ground level have been calculated from the hourly means of fair-weather periods, excluding also hours with any kind of technical faults. The number of accepted hours is almost 32,000 of the 85,000 possible hours in the period. The average seasonal variations show great regularity and can partly be explained by the presence of snow in winter. The diurnal variations are also regular and local influences can be identified in them. The average deviation from Ohm's law is of the order of 10%, that is, the directly measured current density is about 90% of the conduction current calculated as the product of the electric field and the conductivity. This fraction typically varies between 50% and 120% in fair weather, but virtually all of its diurnal and seasonal variations are averaged out during long term.

A loose relation between conductivity and visibility is found which suggests how, in an average sense, certain aerosol properties are associated with different visibility conditions. For example, good visibility is not only associated with low aerosol concentration but also with an aerosol size distribution where the fraction of small particles is relatively high. Yet the small-particle fraction seems to remain modest compared with "standard" continental aerosols in the literature, which means that the aerosol in Finland is mostly aged and gives rise to grey rather than blue haze.

Local influences, such as rush-hour minima on weekdays, are seen in the behaviour of conductivity. The summertime shift of local time by one hour since 1981 is also visible in the results. A tenfold increase in conductivity was caused by the Chernobyl radioactive deposition in April-May 1986; the normal level was reached again by the end of summer 1986.

References

Cerquetti, F., 1988: *Atmospheric electricity data report 1987.* Osservatorio Geofisico Sperimentale, Macerata.

Fleagle, R.G. and Businger, J.A., 1963: *An Introduction to Atmospheric Physics.* Academic Press, New York.

Hoppel, W.A., 1985: Ion-aerosol attachment coefficients, ion depletion, and the charge distribution on aerosols. *J. Geophys. Res.*, **90**(D4), 5917–5923.

Israel, H., 1970: *Atmospheric Electicity, Vol. I.* Israel Program for Scientific Translations, Jerusalem.

Israel, H., 1973: *Atmospheric Electricity, Vol. II.* Israel Program for Scientific Translations, Jerusalem.

Israelsson, S. and Knudsen, E., 1986: Effects of radioactive fallout from a nuclear power plant accident on electrical parameters. *J. Geophys. Res.*, **91** (D11), 11909–11910.

Junge, C., 1963: *Air Chemistry and Radioactivity.* Academic Press, New York.

Lemström, S., in: *Observations Météorologiques faites à Helsingfors* 1890,..,1900; *Meteorologisches Jahrbuch für Finnland* 1901,..,1911.

McCormick, M.P., Lawrence, J.D., Jr., and Crownfield, F.R., Jr., 1968: Mie total and differential backscattering cross sections at laser wavelengths for Junge aerosol models. *Appl. Opt.*, **7**, 2424–2425.

Tuomi, T.J., 1981: Atmospheric electrode effect: approximate theory and wintertime observations. *Pure Appl. Geophys.*, **119**, 31–45.

Tuomi, T.J., 1982: The atmospheric electrode effect over snow. *J. Atm. Terr. Phys.*, **44**, 737–745.

Tuomi, T.J., 1988: Observations of atmospheric electricity 1986. *Geophysical Publications 7*, Finnish Meteorological Institute, Helsinki, 61 p.

Ungethüm, E., Hultberg, A., Israelsson, S., and Knudsen, E., 1974: Die atmosphärisch-elektrischen Grundelemente unter ungestörten Verhältnissen in Marsta - Uppsala. *Gerlands Beitr. Geophysik*, **83**, 19–31.

Van de Hulst, H.C., 1957: *Light Scattering by Small Particles.* Wiley, New York.